International Journal of GEOMATE, April 2019, Vol.16, Issue 56, pp. 1 - 8
ISSN: 2186-2982 (P), 2186-2990 (O), Japan, DOI: https://doi.org/10.21660/2019.56.4550
Special Issue on Science, Engineering & Environment

TIME AND FREQUENCY ANALYSIS OF THE ENGINE SUPPORT VIBRATION WITH HYDROGEN-DIESEL DUAL-FUELING

*Boonthum Wongchai, Poranat Visuwan, Sathaporn Chuepeng

Faculty of Engineering at Sriracha, Kasetsart University, Thailand

*Corresponding Author, Received: 03 Dec. 2018, Revised: 17 Dec. 2018, Accepted: 10 Jan. 2019

ABSTRACT: Hydrogen-diesel dual fuel is used as alternative energy in a diesel engine for saving diesel fuel and protecting the environment. Hydrogen is sustainable, renewable, and carbon-free. It can be produced from various procedures. Hydrogen addition affects engine vibration and car seat vibration. This article presents the effect of hydrogen flow rate on root mean square value and spectrum of the vibration of the engine support. The four-stroke single-cylinder diesel engine is tested with hydrogen-diesel dual fuel by varying hydrogen flow rate. The vibration of the engine support is measured at two constant speeds with three different loads. The root means square and the fast Fourier transform of the engine support vibration are calculated to analyze the vibration signals. The results of the root mean square of the total acceleration show that the root means square value of the engine support vibrations tends to increase by adding the hydrogen flow rate. The fast Fourier transform spectrums in the experimental results show that the average peak acceleration of the first three engine frequencies around 0 to 70 Hz tends to decrease by adding the hydrogen flow rate. The car seat resonance vibration at this frequency range can be reduced by adding the hydrogen flow rate.

Keywords: Hydrogen-diesel dual fuel, Time and frequency analysis, Fast Fourier transform, Vibration

1. INTRODUCTION

In the present days, diesel engines are mainly used in the transportation and the logistic systems. Hydrogen is an alternative essential source of arising in the past decades. It can be produced from various procedures such as water electrolysis, steam reforming, and dehydrogenation of organic chemical hydrides. Diesel engines are nowadays widely used in vehicles and stationary applications. Many researchers study the effect of hydrogen addition on diesel engine performance and pollution [1-5]. Carbon and hydrocarbon emission can be reduced by adding hydrogen to a diesel engine. For the thermal efficiency, hydrogen-diesel dual fuel operation shows higher thermal efficiency than a conventional diesel operation at the condition of relatively high engine load [6].

Hydrogen addition affects cylinder pressure, the vibration of a diesel engine, and noise emission. Nguyen and Mikami [7] studied the effect of hydrogen addition to intake air on combustion noise. The results showed that the combustion noise at late diesel fuel injection greatly decreased by hydrogen addition of 10 vol% while the mean effective pressure was almost the same with or without hydrogen addition. Uludamar et al. [8] reported that the Hydroxyl (the mixture of hydrogen and oxygen gases) addition with diesel-biodiesel blends decreases the engine vibration.

Engine block vibration is produced by shaking force and shaking torque at crankshaft main bearing. At a piston head, gas pressure force pushes a piston and transmits through connecting rod, crankshaft, engine support and other components and produces translational and rotational vibration. By using the Fourier series expansion, the gas pressure force generated within the *i*th cylinder can be computed from

$$M_{gi} = M_{0i} + \sum_{k=1/2}^{K} A_{ki} \cos(k\omega t + \phi_i) + \sum_{k=1/2}^{K} B_{ki} \sin(k\omega t + \phi_i), \quad (1)$$

where M_{0i} is the average torque due to gas forces generated within the *i*th cylinder; A_{ki} and B_{ki} are the coefficients of Fourier series; ω is the engine speed in rad/s; ϕ_i is the initial phase angle; and K = 24 for four-stroke engine [9].

For four-stroke diesel engine, during the compression stroke, diesel oil is injected and fires with the high-temperature air one time per two revolutions of the crankshaft. The first main harmonic frequency of an engine vibration with *i* cylinders can be computed from

$$\mathrm{N} = 120 f / i, \quad (2)$$

where N is the engine speed in RPM and *f* is the first main harmonic frequency in Hz. Time and frequency analysis is mainly used to analyze an engine vibration and acoustic emission such as root mean square (RMS), peak value, fast Fourier transform (FFT), power spectrum density (PSD),

and short-time Fourier transform (STFT) [10-13]. The FFT shows an amplitude of engine vibration at any frequencies and PSD is the power of FFT. The STFT is used to analyze transient vibration signals such as valve impact, injector-pulses, and prompt initial knock detection. Taghizadeh-Alisaraei et al. [14-16] used FFT and STFT to analyze the vibration of the compression ignition engine (CI) with biodiesel-diesel fuel blends and ethanol-diesel fuel blends. For biodiesel-diesel fuel blends, the results showed that D100 and B80 had the lowest vibration and STFT can be used for the real-time knock detection and injection control. In addition, the FFT, and STFT are used in engine noise and vibration analysis [17-19].

Engine support vibration can be separated into the responses of excitation force and torque. The force at the engine support has two components in the longitudinal and lateral direction of the piston travel**.** The vibration at engine support transmits throughout the other car components and finally reach car seats. The vertical and horizontal vibration of the car seat causes of driver and passengers discomfort with low resonance frequencies [20-21]. Qiu and Griffin [22] reported that the resonance frequencies of the fore-aft vibration of the seat pan and the backrest are below 50 Hz.

In this study, the engine support vibration of the hydrogen-diesel dual fuel engine with the variation of hydrogen flow rate injected into the engine intake port is investigated and discussed at two constant speeds with three different loads. The RMS and the FFT are used to analyze the vibration signals**.** The obtained results will be beneficial for vibration diagnostics of hydrogen-diesel dual-fuel engines.

2. MATERIALS AND METHOD

2.1 Test Engine and Vibration Measurement

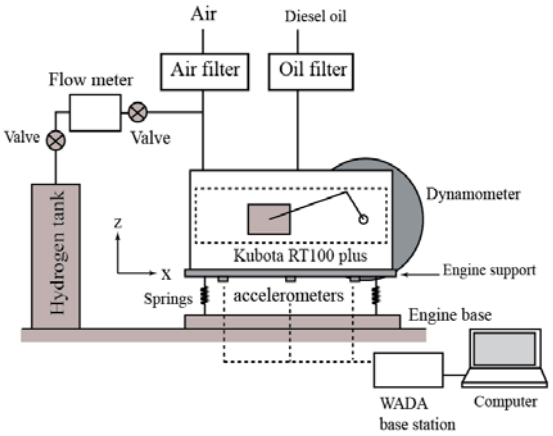

Fig. 1 Test engine and accelerometer installations at engine support (front view).

The horizontal single cylinder Kubota RT100 Plus direct injection diesel engine as shown in Fig.1 is used in this study. The piston moves along x-direction with the connecting rod and the crankshaft move on the x-z plane. The engine is supported by four springs. The specifications of the engine are listed in Table 1.

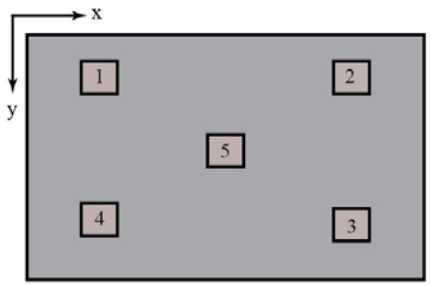

Fig. 2 Accelerometer installations at engine support (bottom view).

Table 1 Engine specification

Model	Kubota RT100 plus
Number of cylinders	1
Bore × stroke	88 mm × 90 mm
Cycle	4-stroke, water cooled
Compression ratio	18:1
Maximum power	7.4 kW at 2,400 rpm
Maximum torque	33.4 Nm at 1,600 rpm
Injection timing	Variable; 20 to 45 degrees BTDC

Table 2 Accelerometer specification

Instrumentation	Characteristics
G-Link	Sample rate: 2,048 samples per channel per second Measuring acceleration: X, Y and Z axes Range: ±2 g or ±10 g Onboard flash memory: 2 MB
WADA base station	Power: USB Frequency: 2.405 GHz to 2.480 GHz

Five G-Link wireless triaxial accelerometers are installed at the bottom of the engine support using

hot glue as shown in Figs. 1 and 2. The engine support acceleration data are stored in onboard flash memory of G-Link accelerometer with the sampling rate of 2,048 samples per second and are transferred to a computer after the tests are completed. G-Link accelerometers are controlled by Node Commander software through WADA base station. The accelerometer specification is listed in Table 2.

2.1 Experimental Test Program

The hydrogen-diesel dual fuel is used in this study. Hydrogen is injected through the flow meter and mixes with air at the manifold with pressure at 1 bar. Hydrogen-air mixture flows into the cylinder during the intake stroke and the main diesel fuel is injected before the piston reaching to TDC during the compression stroke. The hydrogen volume flow rate is varied at five levels of 0, 5, 10, 15 and 20 lpm with the engine speed (N) and the engine load (T) are shown in Table 3. The controlled engine loads are in percentages of the maximum engine torque as described in Table 1. The engine has been set to reach a steady state prior to collecting all data. The engine base accelerations are acquired 100,000 data with sampling rate 2,048 samples per second.

Table 3 Engine parameter

Test program	N (rpm)	T (%)
1	1,600	15
2	1,600	25
3	2,000	25
4	2,000	50

All data are saved in CVS file format. After using FFT, the vibration signals in the frequency domain can be analyzed in the frequency range from 0 to 1,024 Hz. However, for the engine support vibration, this frequency range can be used.

3. RESULT AND DISCUSSION

Time and frequency analysis are used to analyze the vibration data from the accelerometers. The RMS value is used in the time domain. For frequency domain, FFT values are applied in this study using MATLAB.

3.1 Time Analysis of Engine Support Vibration

Figs. 3 and 4 show the RMS values of the total acceleration of the engine support at position 5. From the triaxial accelerometer signals, there are three directions of the acceleration in x, y, and z. The total acceleration can be expressed as

$$a = \sqrt{a_x^2 + a_y^2 + a_z^2}\,, \tag{3}$$

where a_x, a_y, and a_z are the acceleration in x, y, and z-axes. The RMS values of the total acceleration can be computed from

$$\text{RMS} = \sqrt{\frac{1}{n}\sum_{j=1}^{n} a_j^2}\,. \tag{4}$$

The regression analysis is used to investigate the graph trend (dash line) with 2nd polynomial regression. The results show that the RMS value of the engine support accelerations tends to gain up by increasing the hydrogen flow rate with the average R-squared value of 0.86. By leveling up the engine load, the graphs tend to the upside down parabola with the peak at the hydrogen flow rate of 10 lpm. The difference between the RMS values at 1,600 rpm and 2,000 rpm is that the RMS value at 1,600 rpm is decreased by leveling up the engine load while the RMS value at 2,000 rpm is increased. For the RMS value at positions 1 to 4, the graphs are similar to that of position 5.

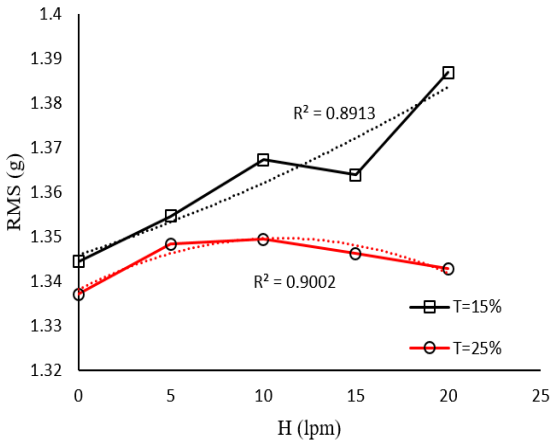

Fig. 3 The RMS at position 5; N = 1,600 rpm

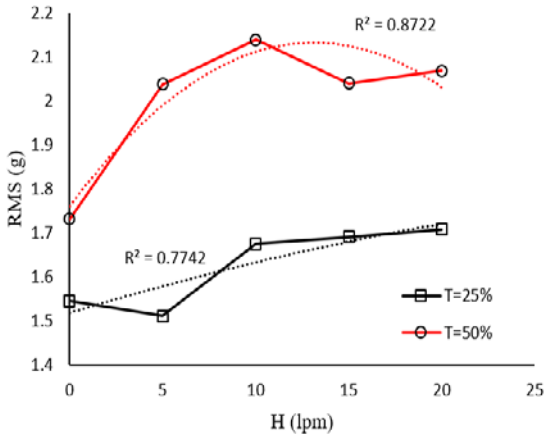

Fig. 4 The RMS at position 5; N = 2,000 rpm

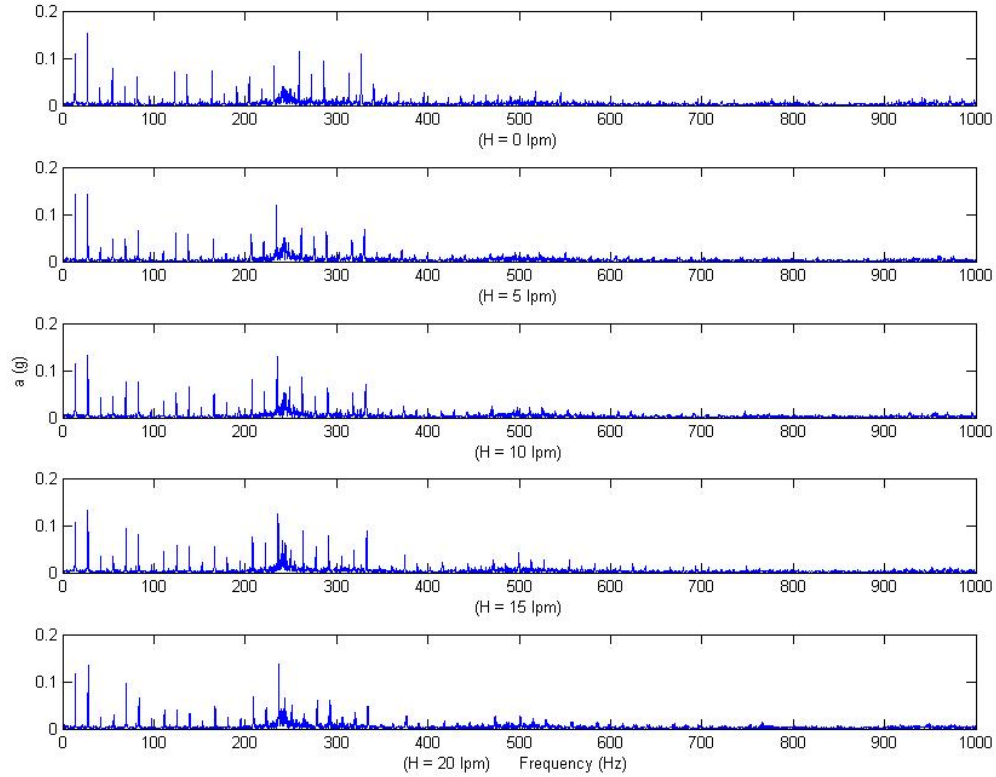

Fig. 5 0 to 1,000 Hz spectrum of the total acceleration at position 5; N = 1,600, T = 25%.

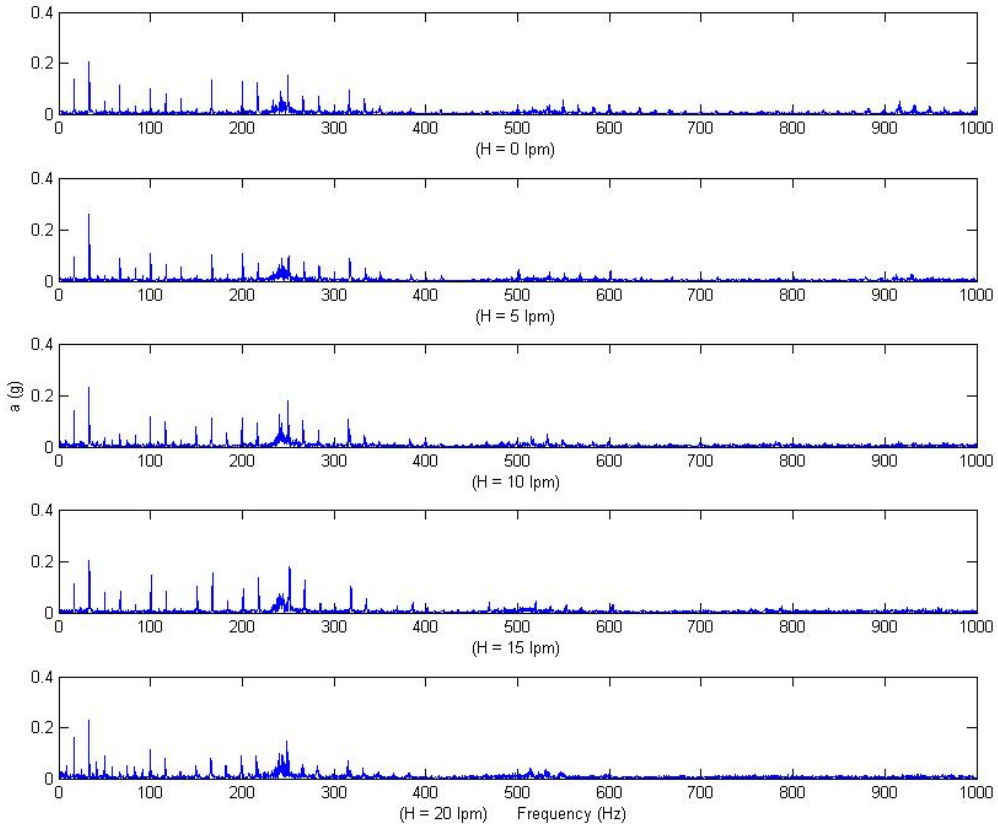

Fig. 6 0 to 1,000 Hz spectrum of the total acceleration at position 5; N = 2,000, T = 25%.

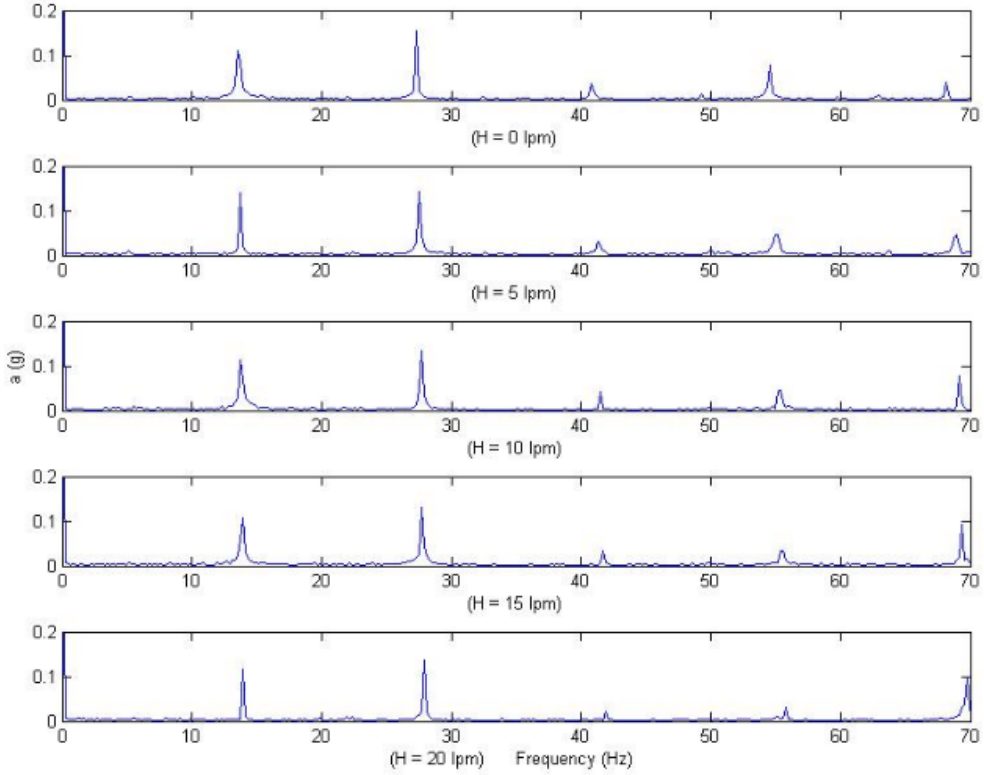

Fig. 7 0 to 70 Hz spectrum of the total acceleration at position 5; N = 1,600 rpm, T = 25%.

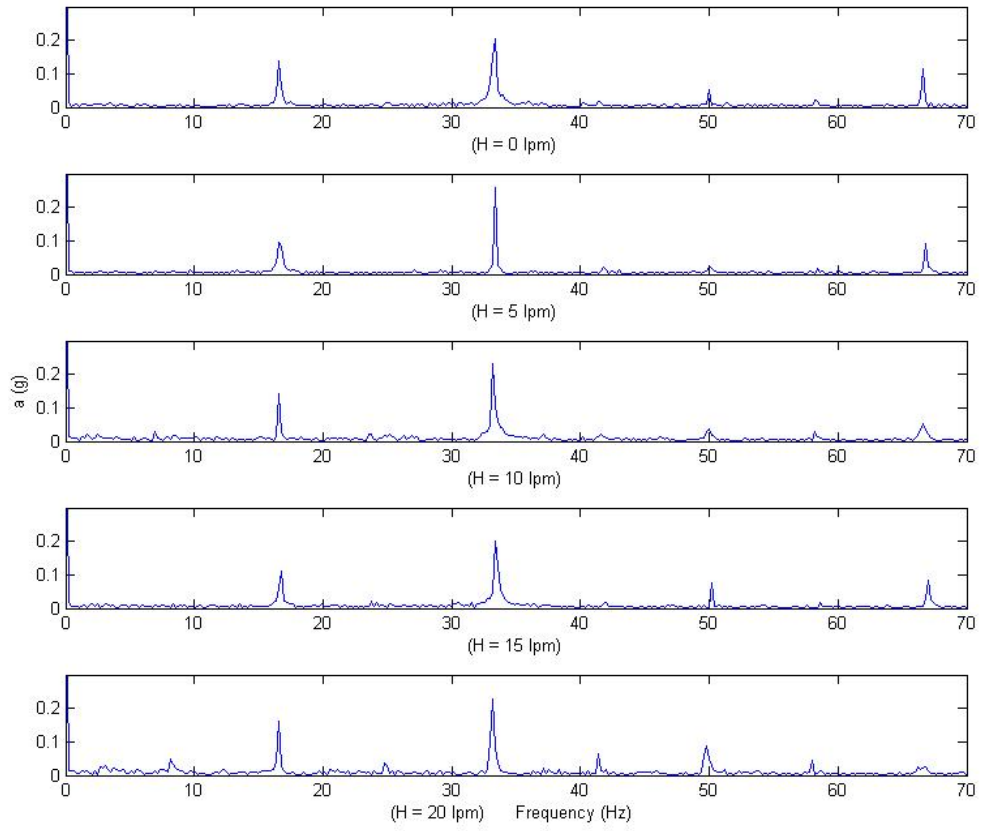

Fig. 8 0 to 70 Hz spectrum of the total acceleration at position 5; N = 2,000 rpm, T = 25%.

3.2 Frequency analysis of Engine Support Vibration

The FFT is used to analyze the engine support vibration. For a discrete signal x[n], the FFT is can be expressed as

$$x[k] = \sum_{n=0}^{M-1} x[n] e^{-j2n\pi k/M}, \quad (5)$$

where n = 0, 1, 2, …, M-1, and M is length of x[n]. For four-stroke single piston diesel engine, the engine vibration is generated by the combustion of the mixture vapor one time per two revolutions .The engine frequency f in Hz can be calculated from $f = \mathrm{N}/(120)$ and the harmonic frequencies are $\mathrm{n} \times f$ where n are 1, 2, 3, 4, etc. The four-stroke engine with the speed of 1600 rpm has the engine frequencies of 13.33, 26.67, 53.33 Hz, etc. For the engine speed of 2,000 rpm, the engine frequencies are 16.67, 33.33, 66.67 Hz, etc.

Figures 5 to 8 show the FFT of the total acceleration of the engine support at position 5 with the engine speed of 1,600 and 2,000 rpm at 25% engine load. Figure 5 and 6 show the frequency range of 0 to 1,000 Hz. The results show that hydrogen addition unclearly affects the engine vibration.

Figures 7 and 8 show the first three dominant engine frequencies around 0 to 70 Hz. These frequencies affect resonance frequencies of the car seat. The resonance vibration of the car seat with high amplitude occurs at the engine frequency below 50 Hz [22] and cause discomfort of driver and passengers. The average amplitude of the first three engine frequencies around 0 to 70 Hz is defined as the average peak acceleration (APA) and can be computed from

$$\mathrm{APA} = (\mathrm{APA}_{f1} + \mathrm{APA}_{f2} + \mathrm{APA}_{f3})/3, \quad (6)$$

where APA_{f1}, APA_{f2}, and APA_{f3} are the amplitudes at the first, the second, and the third harmonic frequency of the engine vibration.

Figures 9 and 10 show that the APA tend to reduce by increasing the hydrogen flow rate. In addition, there are other frequencies generated by other components occur around 0 to 70 Hz. However, the present study interests to discuss only the effect of added hydrogen on the vibration amplitude at the engine frequencies because the engine is the vibration source and added hydrogen directly affects the engine vibration. For the APA at positions 1 to 4, the results similar to the APA at position 5.

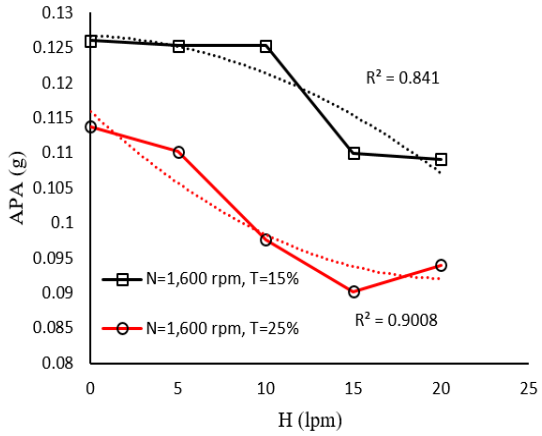

Fig. 9 Average peak of the total acceleration of the first three engine frequencies; N = 1,600 rpm.

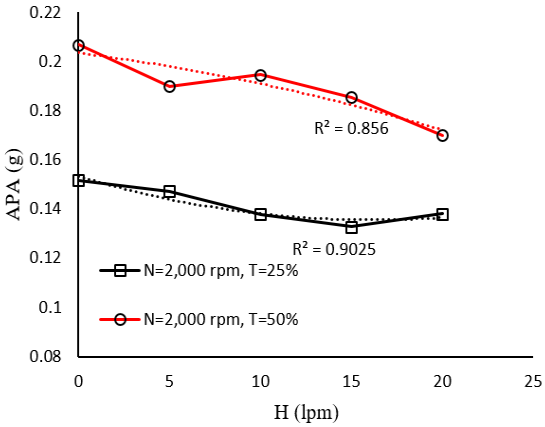

Fig. 10 Average peak of the total acceleration of the first three engine frequencies; N = 2,000 rpm.

4. CONCLUSION

This paper present time and frequency analysis of engine support vibration, the hydrogen-diesel dual fuel engine is tested by varying hydrogen flow rate. The vibration of the engine support is measured at two different speeds and three different loads.

The RMS and the FFT are used to analyze the signals of the engine support vibration. The results found that the RMS value of the engine support vibrations tends to increase by adding the hydrogen flow rate. From the FFT spectrum at the resonance frequencies of the car seat vibration, the added hydrogen flow rate reduces the average peak acceleration of the first three engine frequency around 0 to 70 Hz. For this frequency range, the car seat resonance vibration can be reduced by increasing the hydrogen flow rate.

5. ACKNOWLEDGMENTS

The study was conducted at Kasetsart University Sriracha Campus. The authors would like to thank the Kasetsart University Research and Development Institute (KURDI) for the provision of the research grant to this project under the contract number V-T(D)173.53. The Kasetsart University Center for Advanced Studies in Industrial Technology under the National Research University (NRU) project is also acknowledged for the support to this study.

6. REFERENCES

[1] Shekar R. D., and Purushothama H. R., Hydrogen Induction to Diesel Engine Working on Bio-Diesel: A Review. Procedia Earth and Planetary Science, Vol. 11, 2015, pp. 385-392.

[2] Wu H.W., Hsu T.T., He J.Y., and Fan C.M., Optimal performance and emissions of diesel/hydrogen-rich gas engine varying intake air temperature and EGR ratio, Applied Thermal Engineering, Vol. 124, 2017, 381–392.

[3] Aldhaidhawi M., Chiriac R., Bădescu V., Descombes G., and Podevin P., Investigation on the mixture formation, combustion characteristics and performance of a Diesel engine fueled with Diesel, Biodiesel B20 and hydrogen addition, International Journal of Hydrogen Energy, Vol. 42, Issue 26, 2017, pp. 16793-16807.

[4] Taghavifar H., Anvari S., and Parvishi A., Benchmarking of water injection in a hydrogen-fueled diesel engine to reduce emissions, International Journal of Hydrogen Energy, Vol. 42, Issue 26, 2017, pp. 11962-11975.

[5] Hoseinia S. S., Najafia G., Ghobadiana B., Mamatb R., Sidikc N. A. C., and Azmib W.H., The effect of combustion management on diesel engine emissions fueled with biodiesel-diesel blends, Renewable, and Sustainable Energy Reviews, Vol. 73, 2017, pp. 307–331.

[6] Tsujimura T., and Suzuki Y., The utilization of hydrogen in hydrogen/diesel dual fuel engine, International Journal of Hydrogen Energy, Vol. 42, Issue 19, 2017, pp. 14019-14029.

[7] Nguyen T. A., and Mikami M., Effect of hydrogen addition to intake air on combustion noise from a diesel engine, International Journal of Hydrogen Energy, Vol. 38, Issue 10, 2013, pp. 4153-4162.

[8] Uludamar E., Tosun E., Tüccar G., Yıldızhan S., Çalık A., Yıldırım S., Serin H., and Özcanlı M., Evaluation of vibration characteristics of a hydroxyl (HHO) gas generator installed diesel engine fuelled with different diesel-biodiesel blends, International Journal of Hydrogen Energy, 42, Issue 36, 2017, pp. 23352-23360.

[9] Lin H., and Ding K., A new method for measuring engine rotational speed based on the vibration and discrete spectrum correction technique, Measurement, Vol. 46, Issue 7, 2013, pp. 2056–2064.

[10] Yao J., Xiang Y., Qian S., Li S., and Wu S., Noise source separation of a diesel engine by combining binaural sound localization method and blind source separation method, Mechanical Systems and Signal Processing, Vol. 96, 2017, pp. 303–320.

[11] Moosavian A., Najafi G., Ghobadian B., and Mirsalim M., The effect of piston scratching fault on the vibration behavior of an IC engine, Applied Acoustics, Vol. 126, 2017, pp 91–100.

[12] Barelli L., Bidini G., Bonucci F., and Moretti E., The radiation factor computation of energy systems by means of vibration and noise measurements: The case study of a cogenerative internal combustion engine, Applied Energy, Vol. 100, 2012, pp. 258–266.

[13] Giancarlo C., Ornella C., Fulvio P., and Andrea P., Diagnostic methodology for internal combustion diesel engines via noise radiation, Energy Conversion and Management, Vol. 89, 2015, pp. 34–42.

[14] Taghizadeh-Alisaraei A., Ghobadian B., Tavakoli-Hashjin T., and Mohtasebi S. S., Vibration analysis of a diesel engine using biodiesel and petrodiesel fuel blends, Fuel, Vol. 102, 2012, pp. 414-422.

[15] Taghizadeh-Alisaraei A., Ghobadian B., Tavakoli-Hashjin T., Mohtasebi S. S., Rezaei-asl A., and Azadbakht M., Characterization of engine's combustion-vibration using diesel and biodiesel fuel blends by time-frequency methods: A case study, Renewable Energy, Vol. 95, 2016, pp. 422-432.

[16] Taghizadeh-Alisaraei A., and Rezaei-Asl A., The effect of added ethanol to diesel fuel on performance, vibration, combustion and knocking off a CI engine, Fuel, Vol. 185, 2016, pp. 718–733.

[17] Uludamar E., Tosun E., and Aydın K., Experimental and regression analysis of noise and vibration of a compression ignition engine fuelled with various biodiesels, Fuel, Vol. 177, 2016, pp. 326-333.

[18] Çelebi K., Uludamar E., Tosun E., Yıldızhan S., K., and Özcanlı M., Experimental and Aydın artificial neural network approach of noise and vibration characteristic of an unmodified diesel engine fuelled with conventional diesel, and biodiesel blends with natural gas addition, Fuel, Vol. 197, 2017, pp. 159-173.

[19] Toward M. G.R., and Griffin M. J., The transmission of vertical vibration through seats: Influence of the characteristics of the human body, Journal of Sound and Vibration, Vol. 330,

Issue 26, 2011, pp. 6526–6543.

[20] Qiu Y., and Griffin M.J., Transmission of fore-aft vibration to a car seat using field tests and laboratory simulation, Journal of Sound and Vibration, Vol. 264, Issue 1, 2003, pp. 135–155.

[21] Patel C., Agarwal A. K., Tiwari N., Lee S., Lee C. S., and Park S., Combustion, noise, vibrations and spray characterization for Karanja biodiesel fuelled engine, Applied Thermal Engineering, Vol. 106, 2016, pp. 506–517.

[22] Zhang X., Qiu Y., and Griffin M. J., Transmission of vertical vibration through a seat: Effect of thickness of foam cushions at the seat pan and the backrest, International Journal of Industrial Ergonomics, Vol. 48, 2015, pp. 36-45.